JOURNAL OF GUIDANCE, CONTROL, AND DYNAMICS
Vol. 25, No. 2, March–April 2002

Hybrid Cartesian and Orbit Element Feedback Law for Formation Flying Spacecraft

Hanspeter Schaub*
ORION International Technologies, Albuquerque, New Mexico 87106
and
Kyle T. Alfriend†
Texas A&M University, College Station, Texas 77843

A spacecraft formation flying control strategy is discussed where the desired orbit is prescribed in terms of specific orbit element differences and the relative orbit is measured in terms of Cartesian coordinates of the rotating reference frame centered on the chief satellite. A direct method to map orbit element differences to their corresponding local Cartesian coordinates is presented. A numerical study illustrates the accuracy with which this linearized transformation performs this coordinate transformation. A hybrid continuous feedback control law is then developed that has the desired relative orbit geometry explicitly given in terms of orbit element differences and the actual orbit given in terms of local Cartesian coordinates. A numerical simulation illustrates the performance and limitations of such feedback control laws. Using the linearized mapping between the relative orbit coordinates causes only a small performance penalty. However, it is advantageous to work in mean element space when determining the relative orbit tracking error.

Introduction

FOR formations of geometrically identical spacecraft, the dominant perturbing factor in low Earth orbit is the J_2 gravitational perturbation. For nonidentical spacecraft, the dominant perturbation could be the differential aerodynamic or differential solar radiation force. When describing and controlling formations of geometrically identical spacecraft, it is convenient to do so by describing the periodic relative orbit geometry in terms of relative orbit element differences, rather than using the Cartesian coordinates of the rotating local-vertical–local-horizontal (LVLH) coordinate frame. When the discussion is restricted to a spherical Earth relative motion, all of the orbital element differences are constant except for the true anomaly. The relative motion will be periodic if the semimajor axis difference is zero, otherwise there will be a difference in orbital period, and secular growth will occur. Out-of-plane motion is a result of the difference in right ascension and inclination. The eccentricity difference determines the size of the in-plane 2–1 relative motion. The displacement of the center of this 2–1 ellipse and the phasing of the satellite in the ellipse result from the initial true anomaly and argument of perigee differences. Thus, it is natural to describe the relative motion in terms of orbital element differences. The actual orbit element difference between deputy and chief satellites can be compared at any point of time to their desired values. This greatly facilitates the task of determining any relative orbit errors and correcting them. Note that the naming convention has been assumed here where deputy satellites are flying about a common chief reference point. The chief reference point does not have to be a satellite, it just describes the desired reference orbit of the formation.

Establishing relative orbits using mean orbit element differences has been discussed in Refs. 1–4. As a comparison, if a general periodic relative orbit is described through some Cartesian initial conditions, then the corresponding differential equations must be integrated to obtain the desired Cartesian coordinates of both the deputy and chief spacecraft. For some special cases it is possible to find closed-form solutions to these relative orbits, such as is the case with the elliptic relative orbits obtained using the Clohessy–Wiltshire equations (see Ref. 5) (sometimes also referred to as Hill's equations). However, these special solutions typically require the chief orbit to be circular and the Earth to be perfectly spherical. Using orbit element differences to describe the relative orbit does not suffer from these constraints and is, thus, more easily applied to the general formation flying problem.

However, a relative orbit is typically sensed or measured in terms of LVLH local coordinates or inertial Cartesian coordinates differences and, typically, not directly in terms of orbit element differences. One method to map these local position and velocity measurements into corresponding orbit element differences is to use these local coordinates, along with the inertial position and velocity vectors of the chief, to reconstruct the deputy inertial position and velocity coordinates. These inertial quantities are then mapped uniquely into corresponding orbit elements, which then lead to the desired orbit element differences.

This paper outlines an alternate, more direct approach. By the use of various celestial mechanics properties, a direct mapping between the local Cartesian position and velocity coordinates and the osculating orbit element differences is developed. This transformation is a first-order approximation to the true nonlinear transformation, where it is assumed that the relative orbit dimensions are very small compared to the inertial orbits. As is shown in Ref. 6, the error in the relative motion resulting from linearization is minimized if we use orbital elements. The good accuracy of this direct mapping between orbit element differences and local Cartesian coordinates is illustrated through a numerical simulation. In both Refs. 7 and 8, the development of a similar linear mapping between orbit element differences and small differences in relative position and velocity coordinates is described. The mapping presented in this paper is in terms of orbit elements that lead to nonsingular equations for the circular orbit case. Whereas the previous mappings expressed the relative coordinate rates relative to the true latitude angle, we provide direct expressions for the time rate of change of the relative position vector.

Furthermore, a hybrid continuous feedback control law in terms of both the local Cartesian relative orbit coordinates and the desired orbit element differences is presented. The linear mapping between local Cartesian coordinates and orbit element differences

Presented as Paper 2000-4131 at the AIAA Guidance, Navigation, and Control Conference, Denver, CO, 14–17 August 2000; received 13 November 2000; revision received 17 May 2001; accepted for publication 30 May 2001.

*Research Engineer, 2201 Buena Vista Drive, Suite 211. Member AIAA.
†Department Head and Professor, Aerospace Engineering Department. Fellow AIAA.

will provide a direct method to determine the relative orbit errors at any instant without having to integrate differential equations using the desired relative orbit initial conditions. The accuracy and limitations of such a feedback control law are compared to a similar feedback control law, where the full nonlinear transformation between Cartesian local coordinates and their corresponding orbit elements is utilized. The effect of adding the J_2 gravitational perturbation on the tracking accuracy is also discussed.

Linear Coordinate Mapping

Because the actual relative orbit of a deputy satellite relative to a chief satellite is typically measured or sensed in terms of LVLH Cartesian coordinates, it would be convenient to be able to map these coordinates directly into corresponding orbit element differences. This would greatly facilitate the process of determining relative orbit errors when the desired relative orbit is provided as fixed orbit element differences.

LVLH Position Coordinates

The rotating LVLH coordinate frame has its x axis aligned with the chief's radial position vector and the z axis aligned with the chiefs angular momentum vector. Let the LVLH deputy state vector $\boldsymbol{X}$ be given as

$$\boldsymbol{X} = (x, y, z, \dot{x}, \dot{y}, \dot{z})^T \tag{1}$$

Let a be the semimajor axis, θ be the true latitude angle (sum of argument of perigee and true anomaly), e be the eccentricity, i be the inclination angle, Ω be the ascending node, and ω be the argument of perigee. The orbit element vector $\boldsymbol{e}$ is given through

$$\boldsymbol{e} = (a, \theta, i, q_1, q_2, \Omega) \tag{2}$$

with q_1 and q_2 being defined through

$$q_1 = e\cos\omega \tag{3}$$

$$q_2 = e\sin\omega \tag{4}$$

All coordinates are assumed to be osculating quantities, with the J_2 perturbation not considered at this stage. Because the differences in orbits are small, the deputy orbit element vector is written as

$$\boldsymbol{e}_d = \boldsymbol{e}_c + \delta\boldsymbol{e} \tag{5}$$

A subscript d denotes deputy spacecraft quantities and a subscript c indicates chief spacecraft quantities. Let us define the following three coordinates systems. Let $\mathcal{C}$ and $\mathcal{D}$ be the LVLH coordinate frames of the chief and deputy satellites, respectively, and let $\mathcal{N}$ be the inertial frame. Then $T^{\mathcal{CN}} = T^{\mathcal{CN}}(\Omega_c, i_c, \theta_c)$ is the direction cosine matrix mapping vector components in the inertial frame to components in the chief LVLH frame. To relate the orbit element difference vector $\delta\boldsymbol{e}$ to the corresponding LVLH Cartesian coordinate vector $\boldsymbol{X}$, we write the deputy spacecraft inertial position vector $\boldsymbol{r}_d$ in chief and deputy LVLH frame components as

$${}^{\mathcal{C}}\boldsymbol{r}_d = {}^{\mathcal{C}}(R_c + x, y, z)^T \tag{6}$$

$${}^{\mathcal{D}}\boldsymbol{r}_d = {}^{\mathcal{D}}(R_d, 0, 0)^T \tag{7}$$

where R is the inertial orbit radius. The deputy position vector $\boldsymbol{r}_d$ is now mapped from the deputy LVLH frame vector components to the chief LVLH frame vector components using

$${}^{\mathcal{C}}\boldsymbol{r}_d = T^{\mathcal{CN}}T^{\mathcal{ND}}\,{}^{\mathcal{D}}\boldsymbol{r}_d \tag{8}$$

To simplify the notation from here on, the subscript c is dropped, and any parameter without a subscript is implied to be a chief orbit parameter. Taking the first variation of $T^{\mathcal{ND}}$ and R_d about the chief satellite motion leads to the first-order approximations

$$T^{\mathcal{ND}} \approx T^{\mathcal{NC}} + \delta T^{\mathcal{NC}} \tag{9}$$

$$R_d \approx R + \delta R \tag{10}$$

Equation (8) is then expanded to yield

$${}^{\mathcal{C}}\boldsymbol{r}_d = \left(I_{3\times 3} + T^{\mathcal{CN}}\delta T^{\mathcal{NC}}\right)\begin{pmatrix} R+\delta R \\ 0 \\ 0 \end{pmatrix} \tag{11}$$

Dropping second-order terms, the deputy position vector is written as

$${}^{\mathcal{C}}\boldsymbol{r}_d = \begin{pmatrix} R+\delta R \\ 0 \\ 0 \end{pmatrix} + RT^{\mathcal{CN}}\begin{pmatrix} \delta T_{11}^{\mathcal{NC}} \\ \delta T_{21}^{\mathcal{NC}} \\ \delta T_{31}^{\mathcal{NC}} \end{pmatrix} \tag{12}$$

with the matrix components $\delta T_{i1}^{\mathcal{NC}}$ given by

$$\delta T_{11}^{\mathcal{NC}} = T_{12}^{\mathcal{NC}}\delta\theta - T_{21}^{\mathcal{NC}}\delta\Omega + T_{31}^{\mathcal{NC}}\sin\Omega\,\delta i \tag{13}$$

$$\delta T_{21}^{\mathcal{NC}} = T_{22}^{\mathcal{NC}}\delta\theta + T_{11}^{\mathcal{NC}}\delta\Omega - T_{31}^{\mathcal{NC}}\cos\Omega\delta i \tag{14}$$

$$\delta T_{31}^{\mathcal{NC}} = T_{32}^{\mathcal{NC}}\delta\theta + \sin\theta\cos i\;\delta i \tag{15}$$

When Eqs. (13–15) are substituted into Eq. (12), the deputy position vector is written in terms of orbit element differences as

$${}^{\mathcal{C}}\boldsymbol{r}_d = \begin{pmatrix} R+\delta R \\ 0 \\ 0 \end{pmatrix} + R\begin{pmatrix} 0 \\ \delta\theta + \delta\Omega\cos i \\ -\cos\theta\sin i\delta\Omega + \sin\theta\delta i \end{pmatrix} \tag{16}$$

To be able to write Eq. (16) in terms of the desired orbit elements and their differences, the orbit radius R must be expressed in terms of the elements given in Eq. (2),

$$R = \frac{a\left(1 - q_1^2 - q_2^2\right)}{1 + q_1\cos\theta + q_2\sin\theta} \tag{17}$$

Thus, the variation of R is expressed as

$$\delta R = (R/a)\delta a + (V_r/V_t)R\delta\theta - (R/p)(2aq_1 + R\cos\theta)\delta q_1 - (R/p)(2aq_2 + R\sin\theta)\delta q_2 \tag{18}$$

where the chief radial and transverse velocity components V_r and V_t are defined as

$$V_r = \dot{R} = (h/p)(q_1\sin\theta - q_2\cos\theta) \tag{19}$$

$$V_t = R\dot{\theta} = (h/p)(1 + q_1\cos\theta + q_2\sin\theta) \tag{20}$$

with h being the chief orbit momentum magnitude and p being the semilatus rectum. When the chief LVLH frame components of the deputy position vector descriptions in Eqs. (6) and (16) are compared, the local Cartesian LVLH frame coordinates x, y, and z are expressed in terms of the orbit element differences as

$$x = \delta R \tag{21}$$

$$y = R(\delta\theta + \cos i\delta\Omega) \tag{22}$$

$$z = R(\sin\theta\;\delta i - \cos\theta\sin i\delta\Omega) \tag{23}$$

LVLH Velocity Coordinates

At this point, half of the desired mappings between orbit element differences and the corresponding LVLH Cartesian coordinates have been developed. To derive the linear relationship between the orbit element differences and the Cartesian coordinate rates, a similar approach to that used to derive Eqs. (21–23) could be used. In Ref. 9, the deputy velocity vector is expressed in both the chief and deputy frame. The desired Cartesian coordinate rates are then extracted by comparing the two algebraic expressions.

However, it is also possible to obtain the Cartesian coordinate rate expressions in terms of orbit element differences by differentiating Eqs. (21–23) directly with respect to time. The only time-varying quantities in these three expressions are the chief true latitude θ and the difference between deputy and chief latitude $\delta\theta$. Only the

latter quantity needs special consideration. Using the conservation of angular momentum h, we express the true latitude rate $\dot{\theta}$ as

$$\dot{\theta} = h/R^2 \tag{24}$$

The variation of Eq. (24) yields

$$\delta\dot{\theta} = \delta h/R^2 - 2(h/R^3)\delta R \tag{25}$$

Using the angular momentum expression $h = \sqrt{(\mu p)}$, the δh variation is expressed as

$$\delta h = (h/2p)\delta p \tag{26}$$

where δp is given by

$$\delta p = (p/a)\delta a - 2a(q_1\delta q_1 + q_2\delta q_2) \tag{27}$$

Thus, the desired variation in the true latitude rate is expressed as

$$\delta\dot{\theta} = (h/R^2)[\delta p/2p - 2(\delta R/R)] \tag{28}$$

After differentiating Eqs. (21–23) and making use of Eq. (28), the Cartesian coordinate rates are expressed in terms of orbit element differences as

$$\dot{x} = -(V_r/2a)\delta a + (1/R - 1/p)h\delta\theta + (V_r aq_1 + h\sin\theta) \times (\delta q_1/p) + (V_r aq_2 - h\cos\theta)(\delta q_2/p) \tag{29}$$

$$\dot{y} = -(3V_t/2a)\delta a - V_r\delta\theta + (3V_t aq_1 + 2h\cos\theta)(\delta q_1/p) + (3V_t aq_2 + 2h\sin\theta)(\delta q_2/p) + V_r\cos i\,\delta\Omega \tag{30}$$

$$\dot{z} = (V_t\cos\theta + V_r\sin\theta)\delta i + (V_t\sin\theta - V_r\cos\theta)\sin i\,\delta\Omega \tag{31}$$

Nondimensional Cartesian Coordinates

Even though the feedback control law discussed in this paper requires the dimensional relative Cartesian coordinates and associated time rates, in some applications it is more convenient to work with nondimensional quantities.[7,8] To simplify the following notation, we introduce the nondimensional parameters

$$\alpha = a/R \tag{32}$$

$$\nu = V_r/V_t \tag{33}$$

$$\rho = R/p \tag{34}$$

Let (u, v, w) be the nondimensional relative Cartesian coordinates. When Eqs. (21–23) are divided by the orbit radius R, they are defined as

$$u = x/R = \delta a/a + \nu\delta\theta - (2\alpha q_1 + \cos\theta)\rho\delta q_1 - (2\alpha q_2 + \sin\theta)\rho\delta q_2 \tag{35}$$

$$v = y/R = \delta\theta + \cos i\,\delta\Omega \tag{36}$$

$$w = z/R = \sin\theta\delta i - \cos\theta\sin i\,\delta\Omega \tag{37}$$

Instead of differentiating (u, v, w) with respect to time, we choose to use the true latitude angle θ as the time-dependent variable. Let a prime symbol indicate a derivative with respect to θ. To differentiate the expressions in Eqs. (35–37), only the $\delta\theta$ terms must be given special consideration. Note that

$$\frac{\partial(\delta\theta)}{\partial\theta}\frac{\mathrm{d}\theta}{\mathrm{d}t} = \delta\theta'\dot{\theta} = \delta\dot{\theta} \tag{38}$$

When Eq. (28) is used, the partial derivative of $\delta\theta$ with respect to the true latitude is given by

$$\delta\theta' = \delta p/2p - 2u \tag{39}$$

Taking the partial derivative of Eqs. (35–37) while making use of Eq. (39) yields the following nondimensional rate with respect to true latitude:

$$u' = -\tfrac{3}{2}\nu(\delta a/a) + \left[\rho(q_1\cos\theta + q_2\sin\theta) - \nu^2\right]\delta\theta + (3\nu\alpha q_1 + \sin\theta + \nu\cos\theta)\rho\delta q_1 + (3\nu\alpha q_2 + \cos\theta - \nu\sin\theta)\rho\delta q_2 \tag{40}$$

$$v' = -\tfrac{3}{2}(\delta a/a) - 2\nu\delta\theta + (2\cos\theta + 3\alpha q_1)\rho\delta q_1 + (2\sin\theta + 3\alpha q_2)\rho\delta q_2 \tag{41}$$

$$w' = \cos\theta\delta i + \sin\theta\sin i\,\delta\Omega \tag{42}$$

Note that these nondimensional rate expressions are not simpler that their dimensional counterparts. To map these rates with respect to true latitude into the corresponding dimensional (x, y, z) time rates, the following equations are used:

$$\dot{x} = V_t u' + V_r u \tag{43}$$

$$\dot{y} = V_t v' + V_r v \tag{44}$$

$$\dot{z} = V_t w' + V_r w \tag{45}$$

Linear Mapping Accuracy

Combined, Eqs. (21–23) and (29–31) provide a direct first-order mapping of orbit element differences into corresponding LVLH Cartesian coordinates. These six equations are written in matrix form as

$$\boldsymbol{X} = A(\boldsymbol{e})\delta\boldsymbol{e} \tag{46}$$

where the 6×6 matrix $A(\boldsymbol{e})$ is the linear mapping between the two coordinate sets. To obtain the inverse transformation, the six equations can be solved for $\delta\boldsymbol{e}$ in terms of the $\boldsymbol{X}$ components to yield

$$\delta\boldsymbol{e} = A(\boldsymbol{e})^{-1}\boldsymbol{X} \tag{47}$$

The inverse mapping was developed in Ref. 10 and may be found in the Appendix for completeness.

The following numerical study illustrates what level of errors are introduced to the LVLH Cartesian coordinates when the linear mapping in Eq. (46) is used. Given the chief orbit elements shown in Table 1, specific sets of orbit element differences are used to compute the corresponding LVLH Cartesian position and velocity coordinates.

A semimajor axis, eccentricity, inclination angle, ascending node, argument of perigee, and mean anomaly difference are prescribed individually for each test run. The orbit element differences are swept from zero to a value that corresponds to a relative orbit having a maximum radius of approximately 1 km. The results are shown in Fig. 1.

Note that the semimajor axis causes essentially no transformation errors in the position magnitudes. This result is easily verified analytically. With only the orbit element difference δa being nonzero for this case, using Eqs. (21–23), we find

$$|\boldsymbol{x}| = (R/a)\delta a \tag{48}$$

The chief orbit radius R_c is given by

$$R_c = a_c(1 - e_c\cos E_c) \tag{49}$$

Table 1 Chief orbit elements

Orbit elements	Value	Units
a	7555	km
e	0.05	——
i	48.0	deg
Ω	20.0	deg
ω	10.0	deg
M	120.0	deg

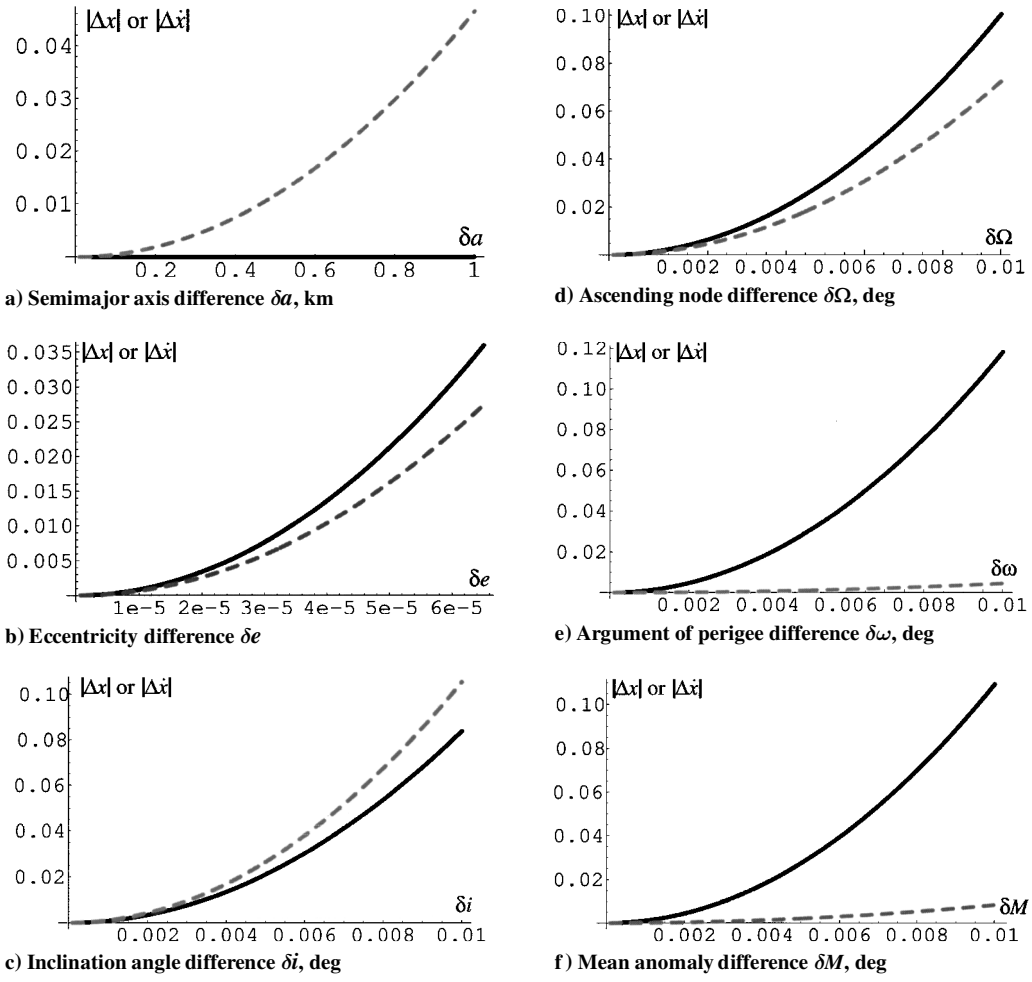

a) Semimajor axis difference δa, km

d) Ascending node difference $\delta\Omega$, deg

b) Eccentricity difference δe

e) Argument of perigee difference $\delta\omega$, deg

c) Inclination angle difference δi, deg

f) Mean anomaly difference δM, deg

Fig. 1 Linear transformation matrix $A(e)$ rms errors mapping orbit element differences to LVLH Cartesian position (——, in meter) and velocity (– – –, in millimeter per second) coordinates.

with E_c being the chief eccentric anomaly. The deputy radius vector is expressed as

$$R_d = (a_c + \delta a)(1 - e_c \cos E_c) = R_c + (R/a)\delta a \qquad (50)$$

because only the semimajor axis is different between chief and deputy satellites for this special case. Here the x coordinate is simply the difference in orbit radii. Thus, the true position vector magnitude is the same as the one predicted by the linear transformation in Eq. (48).

The remaining rms position or velocity errors grow only up to 0.1 m or mm/s, respectively. Considering that for the largest orbit element differences considered here the relative orbit has a radius of about 1 km with relative velocity magnitudes in the meters range, these transformation errors are very small at typically less than 0.1%.

Note that the transformation errors shown are not meant to provide a global bound on the mapping errors. These errors would depend on the chief orbit itself and on the particular orbit latitude angle at which they were evaluated. However, for the given chief orbit with a desired inclination angle difference of the order of 0.01 deg, Fig. 1c shows that any control law that utilizes the linear mapping in Eq. (46) could only expect a final position tracking error of about 0.1 m under the best of circumstances. Using the $A(e)$ mapping instead of the precise nonlinear mapping will result is a small performance loss.

Continuous Feedback Law

Various feedback laws have been proposed for the spacecraft formation flying control task. In Ref. 11, continuous feedback laws are presented in terms of mean orbit element tracking errors and mean inertial Cartesian coordinates tracking errors. Reference 12 presents an impulsive feedback law in terms of mean orbit elements. References 13 and 14 present continuous feedback laws in terms of Cartesian coordinates, and in Ref. 15 a feedback law in terms of orbit elements is discussed.

The use of Eq. (46) is investigated here to create a hybrid continuous feedback control law in terms of Cartesian LVLH frame coordinates and describe the desired relative orbit geometry through a desired set of orbit element differences δe^*. Any desired states are denoted in this paper with a superscript asterisk. The advantage of this type of hybrid control law is that the actual relative orbit is expressed in terms of coordinates in which it would actually be measured, that is, the chief frame local LVLH coordinates, whereas the desired relative orbit is conveniently expressed as a set of orbit element differences.

Let $\boldsymbol{x} = (x, y, z)^T$ be the deputy position vector and $\boldsymbol{v} = (\dot{x}, \dot{y}, \dot{z})^T$ be the deputy velocity vector expressed in the chief LVLH frame. The general linearized relative equations of motion for a Keplerian system are expressed as[16]

$$\dot{\boldsymbol{x}} = \boldsymbol{v} \qquad (51)$$

$$\dot{\boldsymbol{v}} = \underbrace{\begin{bmatrix} 2(\mu/R^3) + \dot{\theta}^2 & \ddot{\theta} & 0 \\ -\ddot{\theta} & \dot{\theta}^2 - \mu/R^3 & 0 \\ 0 & 0 & -\mu/R^3 \end{bmatrix}}_{A_1} \boldsymbol{x} + \underbrace{\begin{bmatrix} 0 & 2\dot{\theta} & 0 \\ -2\dot{\theta} & 0 & 0 \\ 0 & 0 & 0 \end{bmatrix}}_{A_2} \boldsymbol{v} + \underbrace{\begin{pmatrix} u_x \\ u_y \\ u_z \end{pmatrix}}_{\boldsymbol{u}} \qquad (52)$$

These relative equations of motion are valid for both circular and elliptic chief orbits. The latitude acceleration is computed through

$$\ddot{\theta} = -2(\mu/R^3)(q_1 \sin\theta - q_2 \cos\theta) \tag{53}$$

Let us define the relative orbit tracking errors as

$$\Delta \boldsymbol{x} = \boldsymbol{x} - \boldsymbol{x}^* \tag{54}$$

$$\Delta \boldsymbol{v} = \boldsymbol{v} - \boldsymbol{v}^* \tag{55}$$

with the desired position and velocity vectors computed using

$$\boldsymbol{X}^* = \begin{pmatrix} \boldsymbol{x}^* \\ \boldsymbol{v}^* \end{pmatrix} = A(\boldsymbol{e})\delta\boldsymbol{e}^* \tag{56}$$

Note that if the desired orbit element differences call for a fixed mean anomaly difference, as is done in Refs. 1, 11, and 12, then the vector $\delta\boldsymbol{e}^*$ is not constant, but rather $\delta\theta$ must be computed at each instant by solving Kepler's equation. Further, note that $\Delta\dot{\boldsymbol{x}} = \Delta\boldsymbol{v}$.

Let us define the control law $\boldsymbol{u}$ as

$$\boldsymbol{u} = \dot{\boldsymbol{v}}^* - A_1\boldsymbol{x} - A_2\boldsymbol{v} - K\Delta\boldsymbol{x} - P\Delta\boldsymbol{v} \tag{57}$$

with K and P being positive definite matrices. To prove that $\boldsymbol{u}$ is asymptotically stabilizing, a positive definite Lyapunov function V is defined as

$$V(\Delta\boldsymbol{x}, \Delta\boldsymbol{y}) = \tfrac{1}{2}\Delta\boldsymbol{v}^T\Delta\boldsymbol{v} + \tfrac{1}{2}\Delta\boldsymbol{x}^T K\Delta\boldsymbol{x} \tag{58}$$

When Eqs. (52) and (55) are substituted, the derivative of V along the state trajectory must be negative seminegative

$$\dot{V} = \Delta\boldsymbol{v}^T(\Delta\dot{\boldsymbol{v}} + K\Delta\boldsymbol{x}) = -\Delta\boldsymbol{v}^T P\Delta\boldsymbol{v} \tag{59}$$

which guarantees that $\boldsymbol{u}$ is globally stabilizing. To prove that the control law is also asymptotically stabilizing, the higher-order time derivatives of V are investigated. The second derivative of V is zero when evaluated on the set where $\dot{V} = 0$. The third derivative

$$\dddot{V}(\Delta\boldsymbol{v} = 0) = -2\Delta\boldsymbol{x}^T K P K\Delta\boldsymbol{x} \tag{60}$$

is negative definite in the state vector $\Delta\boldsymbol{x}$. Because this first nonzero derivative after $\dot{V}$ is an odd derivative, the control $\boldsymbol{u}$ is asymptotically stabilizing.[17]

Note that $\dot{\boldsymbol{v}}^* - A_1\boldsymbol{x}^* - A_2\boldsymbol{v}^*$ is zero if the desired relative motion is a natural, that is, control free, solution to the linearized equations of motion shown in Eq. (52). When it is assumed that our chosen $\dot{\boldsymbol{v}}^*$ abides by

$$\dot{\boldsymbol{v}}^* = A_1\boldsymbol{x}^* + A_2\boldsymbol{v}^* \tag{61}$$

the control law $\boldsymbol{u}$ is written as

$$\boldsymbol{u} = -[A_1 + K \quad A_2 + P]\left[\begin{pmatrix} \boldsymbol{x} \\ \boldsymbol{v} \end{pmatrix} - A(\boldsymbol{e})\delta\boldsymbol{e}^*\right] \tag{62}$$

Note, however, that the desired relative motion may not necessarily be a natural solution. The control law in Eq. (57) is also valid for forced relative orbits. However, only if the relative orbit is a natural solution will the control vector $\boldsymbol{u}$ go to zero because the desired relative orbit is asymptotically approached. When this form of control law in Eq. (62) is studied, the hybrid nature of $\boldsymbol{u}$ is evident in that the desired relative orbit is prescribed through a set of orbit element differences, whereas the actual motion is expressed in terms of the chief LVLH frame Cartesian components. The advantage here is that we are able to express the actual and desired relative motion in coordinates that best suit their task.

Because the A_2 matrix is skew symmetric, it could be dropped from the control expression in Eq. (62). The Lyapunov-based stability proof remains the same and asymptotic stability is still guaranteed. However, when computing $\dot{V}$ the term $\Delta\boldsymbol{v}^T A_2\Delta\boldsymbol{v}$ is dropped because it is always zero. The modified control expression is then

$$\boldsymbol{u} = -[A_1 + K \quad P]\left[\begin{pmatrix} \boldsymbol{x} \\ \boldsymbol{v} \end{pmatrix} - A(\boldsymbol{e})\delta\boldsymbol{e}^*\right] \tag{63}$$

This control would no longer feedback linearize the closed-loop dynamics, but it still guarantees asymptotic stability.

Note that, whereas the control expression in Eq. (62) takes advantage of the linear mapping $A(\boldsymbol{e})$ between orbit element differences and their corresponding LVLH Cartesian coordinates, the control expression in Eq. (57) does not rely on this mapping. In fact, the relative orbit tracking errors $\Delta\boldsymbol{x}$ and $\Delta\boldsymbol{v}$ could be computed using the complete nonlinear mapping between orbit elements and local Cartesian coordinates. Furthermore, it is possible to incorporate the J_2 effect here by using Brouwer's theory to compute the relative orbit errors in mean element space and then map the error vector back to osculating space for control purposes. The following numerical simulations will demonstrate the performance and limitations of either control law.

Numerical Simulations

The performance of the two continuous feedback control laws in Eqs. (57) and (62) is illustrated through the following numerical simulations. Case 1 uses the simplified control in Eq. (62), which computes the tracking errors in osculating orbit space and takes advantage of the linear mapping between orbit element differences and their corresponding LVLH Cartesian coordinates. Case 2 uses the more general control expression in Eq. (57). Instead of using the linear mapping, the relative orbit errors are computed using the complete nonlinear mapping between orbit elements and Cartesian coordinates. The development of the control law in Eq. (57) makes no assumption on whether the orbit elements and Cartesian coordinates are osculating or mean quantities. Therefore, case 2 uses Brouwer's first-order artificial satellite theory[18] to compute any orbit errors in mean element space. The control in case 2 will, thus, ignore the J_2-induced short-period oscillations and should provide a higher performing control algorithm than case 1.

The chief satellite orbit has the mean orbit elements shown in Table 1. A J_2-invariant relative orbit is designed using the two constraints developed in Refs. 1 and 4. When an inclination angle difference of 0.006 deg, is prescribed, the necessary δa and δe are shown in Table 2. The remaining three orbit element differences are set to zero. Initially, the deputy orbit has a relative orbit error of $\delta a = -0.1$ km, $\delta i = 0.05$ deg, and $\delta\Omega = -0.01$ deg. The position and velocity feedback matrices K and P are replaced with the diagonal matrices with the entries

$$K_{ii} = 0.000032\ \mathrm{s}^{-2}, \qquad P_{ii} = 0.03\ \mathrm{s}^{-1}$$

The numerical simulation solves the nonlinear equations of motion of each satellite including the J_2–J_5 zonal harmonics. The results are shown in Fig. 2. The initial relative orbit tracking error is over 1 km. Figure 2a shows the relative orbit dictated by the desired relative orbit element differences shown in Table 2. This shows the tracking error being essentially canceled after 0.5 orbits. Control cases 1 (solid line) and 2 (dashed line) do not distinguish themselves at this scale, and their performance difference cannot be observed here. Figure 2b shows the magnitude of the relative orbit tracking error on a logarithmic scale. For the first half-orbit, both control cases perform in a nearly identical manner. This portion of the control maneuver is dominated by the feedback portion of the tracking errors. The tracking error for case 1 stabilizes about a mean value in the tens of meters range. The Δv demanded for this two-orbit maneuver is 9.98382 m/s. The tracking error for case 2 decays to a much smaller value of less than 1 m with a commanded Δv of 8.42372 m/s. To isolate the cause for this performance improvement,

Table 2 Deputy orbit element differences

Orbit element difference	Value	Units
δa	−1.92995	m
δe	0.000576727	——
δi	0.00600	deg
$\delta\Omega$	0.0	deg
$\delta\omega$	0.0	deg
δM	0.0	deg

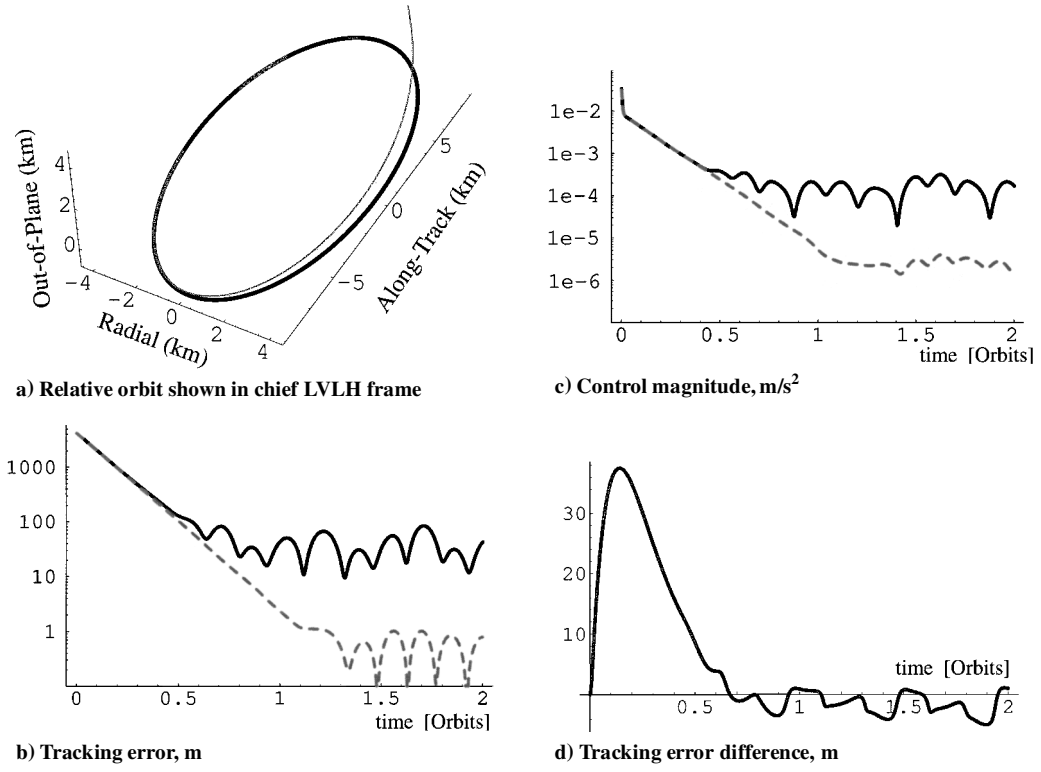

a) Relative orbit shown in chief LVLH frame

c) Control magnitude, m/s^2

b) Tracking error, m

d) Tracking error difference, m

Fig. 2 Simulation results including the J_2–J_5 zonal harmonics.

another case 3 was run, where the nonlinear transformation is used to map orbit element differences into corresponding LVLH Cartesian coordinates, but the tracking errors are computed in osculating element space, not in mean element space as is done in case 2. The tracking error difference between case 1 and this new case 3 is shown in Fig. 2d. Using the nonlinear mapping does result in a slightly better tracking performance initially. However, both cases 1 and 3 stabilize on the same relative orbit tracking error. This indicates that the reduction in final tracking error in case 2 is due to computing the relative orbit tracking error in mean element space. Using the linear mapping $A(\boldsymbol{e})$ instead of the nonlinear mapping thus causes only a relatively minor transient tracking performance loss. To improve the steady-state tracking error, it is necessary to operate in mean element space.

To see the performance of the controls in Eqs. (57) and (62) without the J_2 gravitational perturbation, another set of numerical simulations was performed. No zonal harmonics are included in these simulations. The desired relative orbit is determined through the orbit element differences shown in Table 2, with the exception of $\delta a = 0$ km. This is necessary for the relative orbit not to have a secular drift. A nonzero δa would cause the Keplerian orbits to have different orbit periods. The resulting relative orbit shape is essentially the same as the one shown in Fig. 2a. Note that the only difference between cases 1 and 2 test runs is that case 2 uses the nonlinear mapping between LVLH Cartesian coordinates and orbit element differences. The osculating and mean elements are equal when there are no perturbations. These simulations illustrate the performance penalty of using the $A(\boldsymbol{e})$ matrix under the most ideal circumstances.

Figure 3 shows the simulation results for this Keplerian motion case. Note that the relative orbit tracking errors are reduced to a lower level in case 1 than they were with J_2 gravitational perturbations included. The steady-state tracking errors hover around the 1-m point. The change in velocity Δv requirement for the maneuver in case 1 is $\Delta v = 8.46227$ m/s. If the nonlinear mapping is employed, then the tracking errors asymptotically decay to zero as predicted in the control analysis. The Δv requirement for case 2 is $\Delta v = 8.38649$ m/s.

The linear mapping $A(\boldsymbol{e})$ provides a convenient method to map between the orbit element differences (which describe the relative

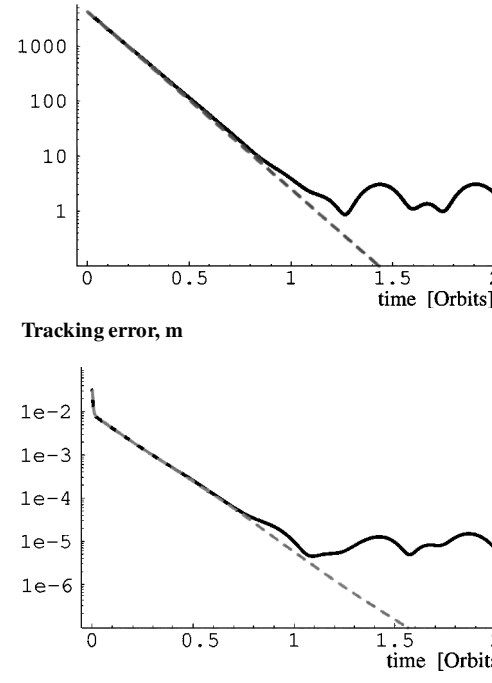

Fig. 3 Simulation results of case 1 (——) and case 2 (- - -) using Keplerian dynamics.

orbit) and the LVLH Cartesian coordinates (which are likely to be the measured quantities). The error introduced through this simplification causes only a small loss in performance of typical control laws.

Conclusions

When describing and controlling natural periodic relative orbits, it is convenient to describe the desired relative orbit geometry in terms of orbit element differences. However, the actual relative orbit of a

deputy satellite relative to a chief satellite will likely be measured in terms of Cartesian coordinates in the rotating chief LVLH frame. A direct linear mapping between the local Cartesian coordinates and the corresponding orbit element differences is outlined here. This mapping is used in the construction of a hybrid continuous feedback control law. The term hybrid is used because the desired orbit is explicitly expressed in terms of orbit element differences and the actual orbit measurements are provided in terms of LVLH Cartesian coordinates. Numerical simulations illustrate that the performance loss due to using the linear mapping is minimal. A more general form of the feedback control law also allows the relative orbit errors to be computed using the full nonlinearities of the relative orbit dynamics. In particular, the nonlinear mapping between Cartesian coordinates and orbit element differences, as well as the transformation from osculating to mean orbit element space, can be incorporated. The latter shows a substantionally improved performance if gravitational perturbations are also considered in the numerical simulation.

Appendix: Inversed $A(e)^{-1}$

The inverse of the matrix $A(\boldsymbol{e})$ is presented.[10] To simplify the expressions, the following notation is introduced:

$$\kappa_1 = \alpha(1/\rho - 1), \qquad \kappa_2 = \alpha\nu^2(1/\rho)$$

The nonzero matrix elements are given by

$$A_{11}^{-1} = 2\alpha(2 + 3\kappa_1 + 2\kappa_2) \tag{A1a}$$

$$A_{12}^{-1} = 2\alpha^2 \nu p / V_t \tag{A1b}$$

$$A_{13}^{-1} = -2\alpha\nu(1 + 2\kappa_1 + \kappa_2) \tag{A1c}$$

$$A_{14}^{-1} = (2a/V_t)(1 + 2\kappa_1 + \kappa_2) \tag{A1d}$$

$$A_{23}^{-1} = 1/R \tag{A1e}$$

$$A_{25}^{-1} = (\cot i/R)(\cos\theta + \nu\sin\theta) \tag{A1f}$$

$$A_{26}^{-1} = -\sin\theta\cot i/V_t \tag{A1g}$$

$$A_{35}^{-1} = (\sin\theta - \nu\cos\theta)/R \tag{A1h}$$

$$A_{36}^{-1} = \cos\theta/V_t \tag{A1i}$$

$$A_{41}^{-1} = (\rho/R)(3\cos\theta + 2\nu\sin\theta) \tag{A1j}$$

$$A_{42}^{-1} = \rho\sin\theta/V_t \tag{A1k}$$

$$A_{43}^{-1} = -(1/R)\left(\rho\nu^2\sin\theta + q_1\sin 2\theta - q_2\cos 2\theta\right) \tag{A1l}$$

$$A_{44}^{-1} = (\rho/V_t)(2\cos\theta + \nu\sin\theta) \tag{A1m}$$

$$A_{45}^{-1} = -(q_2\cot i/R)(\cos\theta + \nu\sin\theta) \tag{A1n}$$

$$A_{46}^{-1} = q_2\cot i\sin\theta/V_t \tag{A1o}$$

$$A_{51}^{-1} = (\rho/R)(3\sin\theta - 2\nu\cos\theta) \tag{A1p}$$

$$A_{52}^{-1} = -\rho\cos\theta/V_t \tag{A1q}$$

$$A_{53}^{-1} = (1/R)\left(\rho\nu^2\cos\theta + q_2\sin 2\theta + q_1\cos 2\theta\right) \tag{A1r}$$

$$A_{54}^{-1} = (\rho/V_t)(2\sin\theta - \nu\cos\theta) \tag{A1s}$$

$$A_{55}^{-1} = (q_1\cot i/R)(\cos\theta + \nu\sin\theta) \tag{A1t}$$

$$A_{56}^{-1} = -q_1\cot i\sin\theta/V_t \tag{A1u}$$

$$A_{65}^{-1} = -(\cos\theta + \nu\sin\theta)/R\sin i \tag{A1v}$$

$$A_{66}^{-1} = \sin\theta/V_t\sin i \tag{A1w}$$

References

[1] Schaub, H., and Alfriend, K. T., "J_2 Invariant Reference Orbits for Spacecraft Formations," NASA Goddard Space Flight Center Flight Mechanics Symposium, Paper 11, May 1999; also *Journal of Celestial Mechanics*, (to be published).

[2] Vadali, S. R., Alfriend, K. T., and Vaddi, S., "Hill's Equations, Mean Orbit Elements, and Formation Flying of Satellites," American Astronautical Society, Paper AAS 00-258, March 2000.

[3] Chichka, D. F., "Dynamics of Clustered Satellites via Orbital Elements," American Astronautical Society, Paper AAS 99-309, Aug. 1999.

[4] Alfriend, K. T., and Schaub, H., "Dynamics and Control of Spacecraft Formations: Challenges and Some Solutions," American Astronautical Society, Paper AAS 00-259, March 2000.

[5] Carter, T. E., "State Transition Matrix for Terminal Rendezvous Studies: Brief Survey and New Example," *Journal of Guidance, Navigation, and Control*, Vol. 31, No. 1, 1998, pp. 148–155.

[6] Junkins, J. L., Akella, M. R., and Alfriend, K. T., "Non-Gaussian Error Propagation in Orbital Mechanics," *Journal of Astronautical Sciences*, Vol. 44, No. 4, 1996, pp. 541–563.

[7] DeVries, J. P., "Elliptic Elements in Terms of Small Increments of Position and Velocity Components," *AIAA Journal*, Vol. 1, No. 9, 1963, pp. 2626–2629.

[8] Garrison, J. L., Gardner, T. G., and Axelrad, P., "Relative Motion in Highly Elliptic Orbits," American Astronautical Society, Paper AAS 95-194, Feb. 1995.

[9] Schaub, H., and Alfriend, K. T., "Hybrid Cartesian and Orbit Element Feedback Law for Formation Flying Spacecraft," AIAA Paper 2000-4131, Aug. 2000.

[10] Alfriend, K. T., Schaub, H., and Gim, D.-W., "Gravitational Perturbations, Nonlinearity and Circular Orbit Assumption Effect on Formation Flying Control Strategies," American Astronautical Society, Paper AAS 00-012, Feb. 2000.

[11] Schaub, H., Vadali, S. R., and Alfriend, K. T., "Spacecraft Formation Flying Control Using Mean Orbit Elements," *Journal of Astronautical Sciences*, Vol. 48, No. 1, 2000, pp. 69–87.

[12] Schaub, H., and Alfriend, K. T., "Impulsive Spacecraft Formation Flying Control to Establish Specific Mean Orbit Elements," American Astronautical Society, Paper AAS 00-113, Jan. 2000.

[13] Kapila, V., Sparks, A. G., Buffington, J. M., and Yan, Q., "Spacecraft Formation Flying: Dynamics and Control," *Proceedings of the American Control Conference*, 1999, pp. 4137–4141.

[14] Middour, J. W., "Along Track Formationkeeping for Satellites with Low Eccentricity," *Journal of Astronautical Sciences*, Vol. 41, No. 1, 1993, pp. 19–33.

[15] Tan, Z., Bainum, P. M., and Strong, A., "The Implementation of Maintaining Constant Distance Between Satellites in Elliptic Orbits," American Astronautical Society, Paper AAS 00-141, Jan. 2000.

[16] Melton, R. G., "Time-Explicit Representation of Relative Motion Between Elliptical Orbits," *Journal of Guidance, Control, and Dynamics*, Vol. 23, No. 4, 2000, pp. 604–610.

[17] Mukherjee, R., and Chen, D., "Asymptotic Stability Theorem for Autonomous Systems," *Journal of Guidance, Control, and Dynamics*, Vol. 16, No. 5, 1993, pp. 961–963.

[18] Brouwer, D., "Solution of the Problem of Artificial Satellite Theory Without Drag," *Astronomical Journal*, Vol. 64, No. 1274, 1959, pp. 378–397.